



P53 introduction enhances chemotherapy-induced apoptosis in HeLa cells

Wei Sun[#], Xiangxuan Zhao[#], Zaiming Lu, Qiyong Guo

Department of Radiology, Shengjing Hospital of China Medical University, Shenyang 110004, China

Contributions: (I) Conception and design: All authors; (II) Administrative support: None; (III) Provision of study materials or patients: None; (IV) Collection and assembly of data: None; (V) Data analysis and interpretation: None; (VI) Manuscript writing: All authors; (VII) Final approval of manuscript: All authors.

[#]These authors contributed equally to this work.

Correspondence to: Qiyong Guo, MD, PhD. Department of Radiology, Shengjing Hospital of China Medical University, 36 Sanhao Street, Heping District, Shenyang 110004, Liaoning, China. Email: guoqy@sj-hospital.org; guoqy@vip.sina.com.cn.

Background: Cervical cancer remains a global health-related issue with over half a million new cases reported annually. However, despite different therapeutic regimens being utilized, over a million women die of cervical cancer each year. This makes it the most lethal cancer and indicates the urgent need for novel therapeutic strategies. This study was to investigate the functional roles of *p53* over-expression in enhancing Lobaplatin (loba)-induced cell growth inhibition and apoptosis in cervical carcinoma cells.

Methods: HeLa cells were treated with recombinant *p53* adenovirus (rAdp53), lobaplatin (loba), or rAdp53 plus loba combination. Subsequently, morphology, Hoechst staining, flow cytometry, and cell proliferation assay were conducted to measure apoptosis and cell growth inhibition *in vitro*. Western blotting was performed to assess protein expression. Xenograft tumor mouse model was used to detect the combined anti-cancer effects of rAdp53 and loba *in vivo*.

Results: *In vitro* assays demonstrated that neither sub-lethal rAdp53 nor loba have any apparent apoptotic effect on HeLa cells. The combination of rAdp53 and loba induced significant apoptosis and cell growth inhibition. *P53* over-expression up-regulated the proapoptotic proteins Bax and Bak. Xenograft cervical tumors derived from HeLa cells demonstrated that co-treatment with rAdp53 and loba effectively inhibited tumor growth *in vivo*.

Conclusions: *P53* restoration can sensitize cervical cancer cells to loba to induce apoptosis and cell growth inhibition.

Keywords: Cervical cancer; *p53*; lobaplatin; chemotherapy; apoptosis

Submitted May 19, 2018. Accepted for publication Aug 15, 2018.

doi: 10.21037/tcr.2018.08.25

View this article at: <http://dx.doi.org/10.21037/tcr.2018.08.25>

Introduction

Cervical cancer (cervical carcinoma, CC), one of the most common gynecological malignancies, remains the second highest cause of cancer-associated morbidity and mortality in women, especially in developing countries such as Asia and Africa (1,2). Currently, neo-adjuvant platinum-based chemotherapy is the most favorable treatment regime for locally advanced cervical cancer. Despite the potency of

chemotherapeutic drugs, CC treatment is rarely curative. Conventional treatments for CC lead to a poor prognosis due to a gradual increase in resistance to chemotherapy (3). There is now compelling evidence demonstrating that the emergence of continuous resistance to chemotherapy-induced apoptosis increases the risk of recurrence and contributes to CC progression or metastasis (4-6). Unfortunately, the biological or pathological elements leading to those transitions are not fully understood.

Therefore, identifying novel molecular targets for overcoming resistance and investigating effective regimes to induce apoptosis in CC has become a primary goal, indispensable for improving and/or developing targeted therapies. Therefore, effective second-line options are urgently needed.

Clinical studies have reported that the human papilloma virus (HPV) is responsible for the occurrence of CC (7,8). The HPV gene product E6 specifically interferes with the cellular tumor suppressor protein *p53*, which results in its inactivation, increasing the probability of cancer formation and serving as a feasible trigger for cell immortalization and transformation (9). Approximately 75% of malignant cervical lesions are associated with *p53* dysfunction induced by HPV16 (a high-risk HPV type) infection (10). Therefore, the status of *p53* is crucial for CC origination, development, and therapy. Restoration of *p53* activity possesses strong therapeutic potential. As an example, Yoon *et al.* demonstrated that TSC-22-mediated inhibition of *p53* proteasomal degradation successfully inhibited cell viability and induced apoptosis in the HPV-positive CC cell lines HeLa and Caski (11). Lee *et al.* further showed that vorinostat-induced acetylation of *p53* enhanced doxorubicin-induced cytotoxicity in HeLa, Caski, and SiHa cells (12). However, another report demonstrated that cisplatin-induced apoptosis was independent of *p53* in HPV-positive HeLa and SiHa cells (13). Consequently, the involvement of *p53* in CC therapy, especially in chemotherapy, remains controversial and needs to be clarified.

In this study, recombinant adenovirus *p53* [rAdp53, Genticine (14,15)] was used in combination with loba to investigate its synergistic anticancer efficacy. We observed that rAdp53 significantly sensitized the loba-induced decrease in cell viability and increase in apoptosis in HeLa cells. rAdp53 infection up-regulated the expression of pro-apoptotic proteins Bax and Bak. Taken together, combined treatment with rAdp53 and loba effectively inhibited tumor growth via apoptosis *in vivo*.

Methods

Cell culture and reagents

HeLa cervical cancer cells were purchased from ATCC (Manassas, VA, USA) and cultivated in DMEM containing high glucose and 10% fetal bovine serum (HyClone, Victoria, Australia) at 37 °C with 5% CO₂. Anti-PARP

polyclonal antibody was purchased from ImmunoWay Biotechnology Company (Newark, DE, USA). Anti-Caspase 8, anti-Caspase 3, anti-Bax, and anti-Bak primary antibodies were obtained from Cell Signaling Technology (Beverly, MA, USA). Anti-GAPDH monoclonal antibody and Hoechst 33258 were obtained from Sigma (St. Louis, MO, USA). Goat anti-rabbit/mouse horseradish peroxidase (HRP)-conjugated secondary antibody was purchased from Santa Cruz Biotechnology (Santa Cruz, CA, USA). Annexin V-PI Apoptosis Detection Kit was obtained from BD Biosciences.

Cell proliferation assays

Cell proliferation (viability) assays were performed as previously described by [3-(4,5-dimethylthiazol-2-yl)-5-(3-carboxymethoxyphenyl)-2-(4-sulfophenyl)-2H-tetrazolium], MTS[®] (16). Briefly, cells were treated with or without desired conditions. Cell viability was determined using the CellTiter[®]96 AQueous One Solution Cell proliferation assay kit according to the supplier's protocol (Promega, WI, USA).

Western blotting

Western blotting was performed to measure protein contents as described previously, with minor modification (17). The cells or tumor tissues were treated and collected, and they were lysed with Nonidet P-40 (1% v/v) lysis buffer containing a protease inhibitor cocktail. After centrifugation at 12,000 rpm for 10 min at 4 °C, the supernatant was collected to prepare cell lysates. The total protein concentration was determined using the Bradford assay. Equivalent amounts of total proteins (20 µg) were loaded, separated by 12% SDS-PAGE gels, and transferred to PVDF membranes. The membranes were blocked with 5% non-fat milk for 30 min, followed by probing with the desired primary antibodies for 2 h at an ambient temperature. After washing three times for 10 min each with 1× PBST, the PDVF membranes were incubated with the appropriate HPR-conjugated secondary antibody. Immunoreactive bands were demonstrated using ECL reagents (Pierce, Rockford, IL, USA). The molecular weight of the protein of interest was assessed using prestained protein markers (Bio-Rad, Hercules, CA, USA). To quantify the Western blot results, the image processing and analysis in Java software (Image J) was used to assess the relative band intensity (RBI) (*vs.* control).

Hoechst staining

Apoptosis was assessed by nuclei morphological changes based on Hoechst 33258 dye staining. Briefly, 5×10^4 cells were seeded into 6-well plates. After treatment with various conditions, Hoechst 33258 (10 mg/mL) was added into the culture medium, followed by further incubation for 15–30 min in an incubator. Apoptotic nuclei were analyzed using an inverted fluorescence microscope (Nikon, Japan). To count the number of apoptotic cells and calculate the apoptotic ratio, six to eight randomly selected areas under the objective lens were counted for the number of apoptotic cells with condensed nuclei or fragmented DNA.

Flow cytometry

Apoptotic cells were characterized with phosphatidylserine (PS) exposure on the outer cell membrane. Apoptosis was examined by flow cytometry based on Annexin V-PI double staining as described previously (18). Briefly, after cells were treated with desired conditions, cells were harvested and stained with fluorescent probes (Annexin V-FITC, green; PI, red). Health cells showed FITC and PI double-negative staining, early apoptotic cells showed FITC-positive and PI-negative staining, and later apoptotic cells were FITC and PI double-positive. Cell sorting was performed using a Flow cytometry (BD Calibur, USA) and analyzed with CellQuest software (BD).

Tumor suppression in vivo

Twenty 6–8-week-old female BALB/c-nu/nu mice were locally bred and used for implantation. They were housed under specific pathogen-free (SPF) conditions with ad libitum access to food and water supply. The mice with 22–25 g net weight were divided into four groups. Further, 1×10^6 control Hela cells or rAdp53-infected Hela cells in PBS or saline were injected subcutaneously into the right flank of all test mice for xenograft tumors ($n=5$ mice/group). When the tumor volume reached around 100 mm^3 (the tumor volume was determined as $v = 1/2ab^2$ with a digital caliper), mice were treated with desired conditions. After treatment, mice were anesthetized, and the tumor was excised from treated or untreated mice and photographed. After the tumor masses were weighed, tissues from different treatment groups were processed for Western blotting to analyze apoptosis and p53 expression.

Statistical analysis

The experiments were repeated at least three times for MTS, flow cytometry, and Western blotting assays. Consistent data were collected, and representative results were shown. Data were expressed as the mean \pm standard error (SE). Significance comparisons among different groups were calculated using one-way ANOVA and the Student's *t*-test. $P < 0.05$ was considered to be statistically significant.

Results

rAdp53 enhances loba-induced apoptotic morphological changes in Hela cells

To investigate the effects of rAdp53, loba, or rAdp53 and loba on cancer cell proliferation, Hela cells were treated with rAdp53, loba, or rAdp53 and loba for 48 h. Cell death was measured through morphology, either under a phase-contrast inverted microscope or fluorescence microscope based on Hoechst 333258 staining. In comparison with controls, rAdp53, or loba single treatment, we found that only the combination of rAdp53 and loba induced significant apoptosis (*Figure 1*). These data suggest that loba induces more apoptosis in the presence of p53 over-expression.

rAdp53 enhances loba-induced cell growth inhibition in Hela cells

To examine whether rAdp53 could enhance the decrease in loba-induced cell viability in CC cells, Hela cells were treated with rAdp53, loba, or rAdp53 plus loba for 48 h. Relative cell viability was assessed through MTS assays. Our results showed that rAdp53 pretreatment markedly inhibited cell viability in Hela cells (*Figure 2*). These data suggest that p53 is able to act synergistically with loba to induce inhibition of cell growth.

Quantitative analysis of apoptosis induced by loba and rAdp53

To further evaluate the apoptosis induced by the combined rAdp53 and loba treatment, cells were treated with rAdp53, loba, or rAdp53 plus loba. Annexin V-PI double staining was performed for flow cytometry. Our data showed that the combined rAdp53 and loba treatment induced markedly more apoptosis than either single treatment in Hela cells (*Figure 3*).

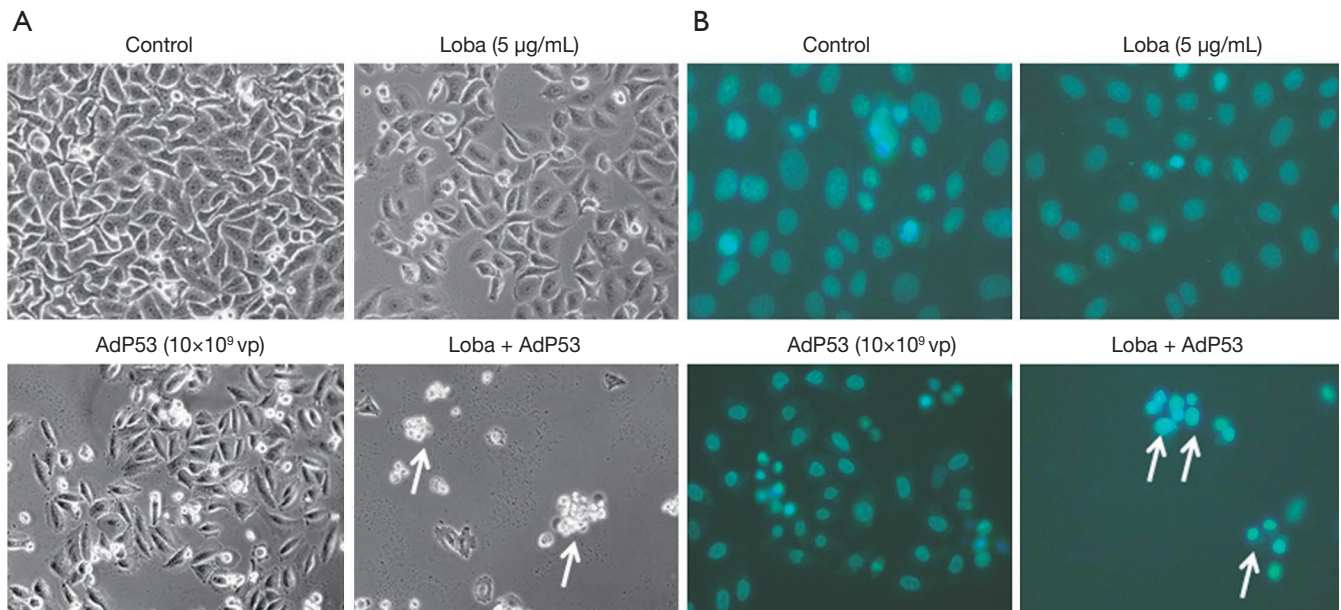


Figure 1 rAdp53 enhances loba-induced apoptosis in HeLa cells. (A) 1×10^5 cells cultivated in 6-well plates were untreated or treated with rAdp53, loba, or rAdp53 plus loba as indicated. Morphological changes were observed under phase-contrast microscopy. White arrows mark representative apoptotic cells; (B) HeLa cells were untreated or treated with rAdp53, loba, or rAdp53 plus loba, and apoptosis was measured via DNA fragmentation or nuclear condensation based on Hoechst 33258 dye staining. White arrows mark representative apoptotic cells (magnification: $\times 200$).

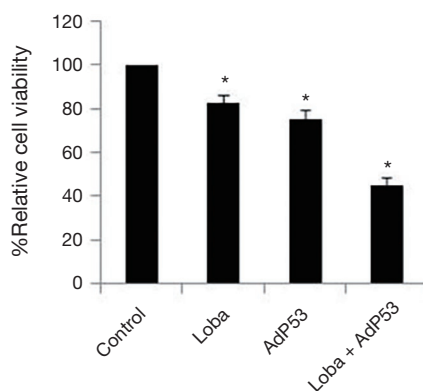


Figure 2 rAdp53 sensitizes loba-induced cell growth inhibition in HeLa cells. (A) HeLa cells cultivated in 96-well plates were untreated or treated with rAdp53 (Adp53, 10×10^9 vp), loba ($5 \mu\text{g/mL}$), or rAdp53 plus loba for 48 h. The MTS assay was performed to assess inhibition of cell growth inhibition effects (*, $P < 0.05$). MTS, [3-(4,5-dimethylthiazol-2-yl)-5-(3-carboxymethoxyphenyl)-2-(4-sulfophenyl)-2H-tetrazolium], MTS[®].

Effects of rAdp53 and loba combined treatment on apoptotic protein expression in HeLa cells

To further assess apoptosis induced by the combined rAdp53 and loba treatment, intracellular apoptotic molecular biochemical events were examined. HeLa cells were untreated or treated with rAdp53, loba, or rAdp53 plus loba for 48 h. Western blotting results demonstrated that loba incubation triggered significant much higher cysteine-aspartic protease (Caspase) and Poly (ADP-ribose) polymerase (PARP) cleavage activation in rAdp53-infected cells (Figure 4). To investigate the mechanism of rAdp53-enhanced loba-induced apoptosis in CC cells, HeLa cells were treated with different concentrations of p53 virus particles (vp) for 48 h. Our data indicated that the pro-apoptotic proteins Bcl-2-associated X protein (Bax) and Bcl-2 homologous antagonist killer (Bak) were significantly up-regulated by rAdp53 infection (Figure 5). These data suggest that p53 may enhance loba-induced apoptosis in HeLa cells through up-regulation of pro-apoptotic proteins.

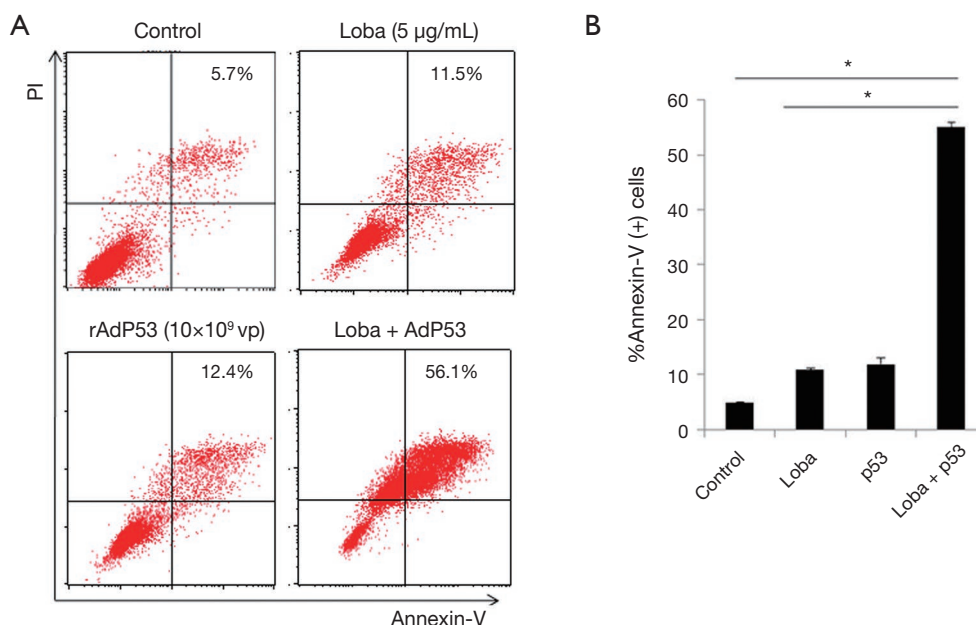


Figure 3 Percentage of apoptotic cells induced by rAdp53 and loba. (A) Cells cultivated in 6-well plates were untreated or treated with rAdp53, loba, or rAdp53 plus loba for 48 h. All cells were harvested, processed, and subjected to flow cytometry based on Annexin-V-PI double staining. Flow cytometry was performed to analyze apoptosis occurrence; (B) statistical analysis was performed to calculate the ratio of (A) (*, $P < 0.05$).

Loba and rAdp53 combination induces tumor growth inhibition

To verify the *in vitro* findings based on cellular tests, tumor inhibition efficacies in terms of tumor volumes and masses in xenograft mice were assessed. Analysis of CC xenograft tumors from the control buffer, rAdp53, loba, or loba plus rAdp53-treated mice revealed that the combined administration of loba and rAdp53 effectively inhibited CC tumor growth *in vivo* (Figure 6A). Excised tumor weight analysis indicated that there was a marked difference in tumor mass with at least a 4-fold decrease in the combination-treated mice when compared with untreated control or single-treated mice (Figure 6B). Moreover, tumor tissues from different treatment groups were processed for Western blotting to examine p53 and cleaved Caspase 3 protein levels. Our results indicated that only the combination treatment significantly induced Caspase 3 activation in the xenograft CC tumors (Figure 6B). These data suggest that loba and rAdp53 indeed synergistically exert anti-cancer therapeutic effects *in vivo*.

Discussion

Besides breast cancer, CC is the most common cause of cancer-related death in women worldwide. Radical surgery management of early-stage cervical carcinoma, including radical hysterectomy (RH), laparoscopic radical hysterectomy (LRH), or laparoscopic nerve-sparing radical hysterectomy (LNRH), has been developed and is routinely used clinically (19-21). However, for advanced stage cervical carcinoma, metastasis and recurrence are the main impediments that prevent cures of this malignancy. The standard of care for advanced cervical cancer has been RH followed by systemic chemotherapy: neoadjuvant chemotherapy (NAC) (22,23). The benefits and risks of NAC to treat locally advanced cervical cancer remain to be determined. Lobaplatin, as the third-generation platinum and the first-line chemotherapeutic strategy for a wide range of preclinical tumor models, exhibits efficacies to neutralize resistance of some types of malignancies to cisplatin or carboplatin (24). Lobaplatin has shown forceful anti-neoplasm ability and has been used in NAC

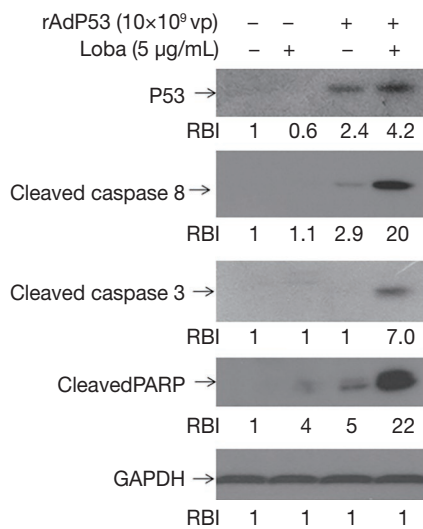


Figure 4 Caspase activation in rAdp53 and loba-treated HeLa cells. HeLa cells seeded in 25 cm² flasks were untreated or treated with rAdp53, loba, or rAdp53 plus loba for 48 h. All cells were harvested, and lysates were prepared and subjected for Western blotting to evaluate the contents of cleaved Caspase 3, cleaved Caspase 8, cleaved PARP, and p53. Glyceraldehyde 3-phosphate dehydrogenase (GAPDH) levels were detected as an internal total protein equal-loading control. RBI was analyzed by the Image J software to quantify the Western blots. RBI, relative band intensity.

to treat solid tumors, including breast cancer, liver cancer, and lung cancer (25–27). However, there are few studies on lobaplatin's neoadjuvant chemotherapeutic effects on cervical carcinoma. In the present study, we demonstrated that rAdp53 and loba synergistically exert anti-cancer effects in CC. rAdp53 enhanced loba-induced apoptosis and cell growth inhibition. rAdp53 introduction up-regulates expression of the Bcl-2 family proapoptotic proteins Bax and Bak. The results imply that rAdp53 may collaborate with loba to inhibit xenograft cervical tumor growth *in vivo*.

We initially tested the apoptotic effects of either agent alone by treating HeLa cells with different concentrations of loba (0, 1, 2.5, 5.0, 10, and 20 µg/mL) or rAdp53 (0, 2.5, 5.0, and 10×10⁹ vp) (data not shown). Our data indicated that HeLa cells were relatively resistant to low concentrations of loba (≤5 µg/mL). These findings are consistent with some previous studies that cancer cells are not sensitive to low doses of loba (≤10 µg/mL) (28). However, they are in contrast with other reports that found cancer cells are sensitive to low doses of loba (≤5 µg/mL) (29). To investigate the mechanism underlying this apoptotic resistance, we

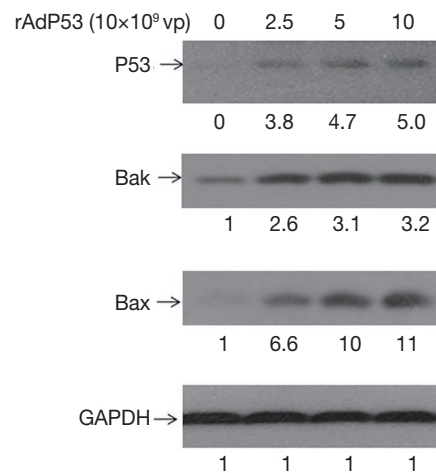


Figure 5 Apoptotic proteins expression in rAdp53-treated HeLa cells. HeLa cells cultivated in 6-well plates were treated with different concentrations of Adp53 (0, 2.5, 5.0, and 10×10⁹ vp) for 48 h. Cells were harvested, and lysates were processed and subjected for Western blotting to assess the contents of p53, Bax, and Bak proteins. GAPDH levels were detected using a total protein equal-loading control. RBI was analyzed by the Image J software to quantify the Western blots. RBI, relative band intensity; vp, virus particles.

infected cells with adenovirus harboring the *p53* gene that produces rAdp53. We found that low concentrations of rAdp53 (≤10⁹ vp) were relatively safe for HeLa cells. Interestingly, our data revealed that pretreatment of HeLa cells with rAdp53 markedly increased their sensitivity to loba-induced apoptosis. These data suggest that *p53* plays a key role in mediating loba-induced apoptosis in CC cells. It is well known that the high-risk HPV oncoprotein E6 can interfere with tumor suppressor *p53* function by promoting its ubiquitylation and proteasomal degradation or by inducing a *p53* mutation. Here, we provide solid data that reveals the *p53* restoration in CC cells sensitizes cells to loba-induced cytotoxicity, suggesting that rAdp53 could be considered as a co-treatment for patients with CC that are treated clinically with loba. These findings are also in agreement with previous reports that loba can exert anti-cancer effects on liver cancer via a *p53*-mediated apoptotic axis (30). It has been reported that *p53* can activate the Bcl-2 family protein Bad to mediate doxorubicin-induced cytotoxicity in cervical cancer (31). To further clarify the mechanism underlying *p53*-sensitized apoptosis induced by loba, our Western blotting data indicated that rAdp53 promoted expression of two other Bcl-2 family proapoptotic proteins, Bax and Bak, in CC cells. Since

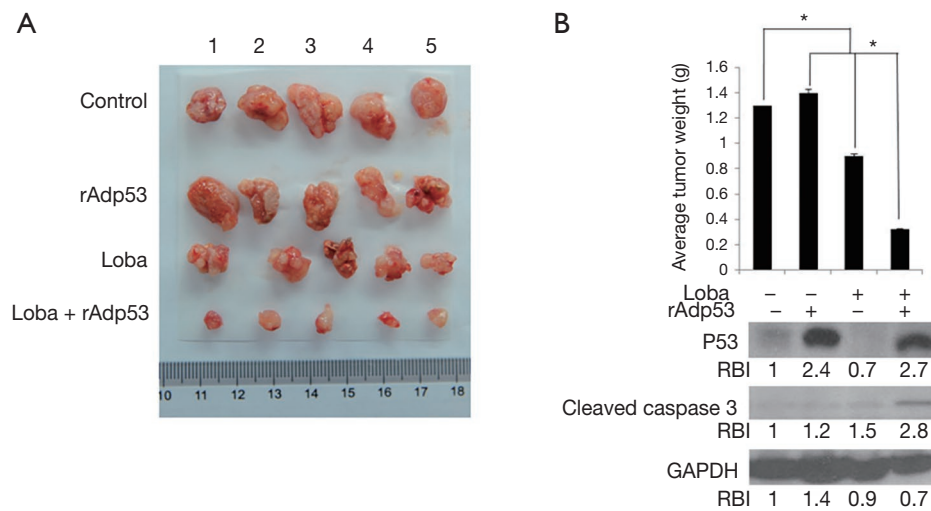


Figure 6 rAdp53 enhanced loba-induced tumor growth inhibition. (A) BALB/c-nu/nu mice were injected subcutaneously with 1×10^6 HeLa cells or HeLa cells harboring rAdp53 in 100 μ L sterile PBS. The mice were untreated or treated with loba (15 mg/kg) via tail vein injection every day for 14 days. After a 2-week treatment, mice were euthanized, and tumors were extracted and photographed; (B) the mass of tumors in nude mice from the control group and groups treated with different conditions were weighted. Statistical analysis was performed to show the inhibitory effects of the different treatments on implanted tumors in nude mice (top panel, *, $P < 0.05$). In addition, tissues excised from untreated and treated tumors were collected, and lysates were prepared and subjected for Western blotting analysis to detect p53 and cleaved Caspase-3 levels using specific antibodies. GAPDH protein levels were assessed and established as an internal equal protein loading control. RBI was analyzed by the Image J software to quantify the Western blots. RBI, relative band intensity.

Bax and Bak can be activated through oligomerization and relocate to the mitochondria, these findings suggest that rAdp53 and loba might trigger an intrinsic apoptotic signaling pathway. Our data support the notion that the chemotherapy drug cisplatin-induced apoptosis in non-small-cell lung cancer (NSCLC) cells is dependent on p53-mediated Bax/Bak activation (32). Secondly, using a SCID mouse model burdened with CC derived from HeLa cells, we observed that treatment with rAdp53 and loba combined significantly inhibited tumor growth *in vivo*, suggesting that over-expression of p53 can indeed play a vital role in CC chemotherapy. The Western blotting results further demonstrated that p53 introduction sensitized loba-induced Caspase 3 cleaved activation. Therefore, the tumor growth inhibitory effects induced by these two agents are based on stimulation of apoptosis *in vivo*.

Conclusions

The study showed that rAdp53 enhanced the ability of loba to induce apoptosis via upregulation of the proapoptotic proteins Bax and Bak. It further demonstrated that this

synergistic anticancer effect via apoptosis functions *in vivo*. Nevertheless, we have acknowledged that more cell lines and primary cells from patients are necessary, which is one of the limitations of this study. This study is only one part of our ongoing novel therapeutic regimes development projects for cervical cancer. We will conduct additional clinical studies to improve the evaluation of this combination in the future. Further investigation is needed to elucidate the toxicity and/or safety of this drug combination for other organs.

Acknowledgments

Funding: This work was supported by the National Science and Technology Major Projects for Major New Drugs Innovation and Development of China (2012ZX09303015 to Q Guo) and the National Natural Science Foundation of China (31371425 to X Zhao and 81771947 to Z Lu).

Footnote

Conflicts of Interest: All authors have completed the ICMJE

uniform disclosure form (available at <http://dx.doi.org/10.21037/tcr.2018.08.25>). The authors have no conflicts of interest to declare.

Ethical Statement: The authors are accountable for all aspects of the work in ensuring that questions related to the accuracy or integrity of any part of the work are appropriately investigated and resolved. This study was performed according to protocols approved by the Committee for Animal Experiments Guidelines on Animal Welfare of the China Medical University Shengjing Hospital (Shenyang, Liaoning, China).

Open Access Statement: This is an Open Access article distributed in accordance with the Creative Commons Attribution-NonCommercial-NoDerivs 4.0 International License (CC BY-NC-ND 4.0), which permits the non-commercial replication and distribution of the article with the strict proviso that no changes or edits are made and the original work is properly cited (including links to both the formal publication through the relevant DOI and the license). See: <https://creativecommons.org/licenses/by-nc-nd/4.0/>.

References

- Nogueira-Rodrigues A, de Melo AC, Garces AH, et al. Patterns of Care and Outcome of Elderly Women Diagnosed With Cervical Cancer in the Developing World. *Int J Gynecol Cancer* 2016;26:1246-51.
- Martinez-Nava GA, Fernandez-Nino JA, Madrid-Marina V, et al. Cervical Cancer Genetic Susceptibility: A Systematic Review and Meta-Analyses of Recent Evidence. *PLoS One* 2016;11:e0157344.
- Boussios S, Seraj E, Zarkavelis G, et al. Management of patients with recurrent/advanced cervical cancer beyond first line platinum regimens: Where do we stand? A literature review. *Crit Rev Oncol Hematol* 2016;108:164-74.
- Sadalla JC, Andrade JM, Genta ML, et al. Cervical cancer: what's new? *Rev Assoc Med Bras (1992)* 2015;61:536-42.
- Cai L, Wang Z, Liu D. Interference with endogenous EZH2 reverses the chemotherapy drug resistance in cervical cancer cells partly by up-regulating Dicer expression. *Tumour Biol* 2016;37:6359-69.
- Ferrandina G, Lauriola L, Distefano MG, et al. Increased cyclooxygenase-2 expression is associated with chemotherapy resistance and poor survival in cervical cancer patients. *J Clin Oncol* 2002;20:973-81.
- Street D, Delgado G. The role of p53 and HPV in cervical cancer. *Gynecol Oncol* 1995;58:287-8.
- Ngan HY, Stanley M, Liu SS, et al. HPV and p53 in cervical cancer. *Genitourin Med* 1994;70:167-70.
- Akeel RA. Identification of HPV Integration and Genomic Patterns Delineating the Clinical Landscape of Cervical Cancer. *Asian Pac J Cancer Prev* 2015;16:8041-5.
- Wu G, Liu D, Jiang K, et al. PinX1, a novel target gene of p53, is suppressed by HPV16 E6 in cervical cancer cells. *Biochim Biophys Acta* 2014;1839:88-96.
- Yoon CH, Rho SB, Kim ST, et al. Crucial role of TSC-22 in preventing the proteasomal degradation of p53 in cervical cancer. *PLoS One* 2012;7:e42006.
- Lee SJ, Hwang SO, Noh EJ, et al. Transactivation of bad by vorinostat-induced acetylated p53 enhances doxorubicin-induced cytotoxicity in cervical cancer cells. *Exp Mol Med* 2014;46:e76.
- Michnov O, Solomayer E, Fehm T, et al. Knock down of p53 or its ubiquitin ligase E6AP does not affect the sensitivity of human papillomavirus-positive cervical cancer cells to cisplatin. *Am J Cancer Res* 2012;2:309-21.
- Peng Z. Current status of gendicine in China: recombinant human Ad-p53 agent for treatment of cancers. *Hum Gene Ther* 2005;16:1016-27.
- Wilson JM. Gendicine: the first commercial gene therapy product. *Hum Gene Ther* 2005;16:1014-5.
- Zheng D, Cho YY, Lau AT, et al. Cyclin-dependent kinase 3-mediated activating transcription factor 1 phosphorylation enhances cell transformation. *Cancer Res* 2008;68:7650-60.
- Zhao X, Liu Y, Du L, et al. Threonine 32 (Thr32) of FoxO3 is critical for TGF-beta-induced apoptosis via Bim in hepatocarcinoma cells. *Protein Cell* 2015;6:127-38.
- Zheng Y, Shi Y, Tian C, et al. Essential role of the voltage-dependent anion channel (VDAC) in mitochondrial permeability transition pore opening and cytochrome c release induced by arsenic trioxide. *Oncogene* 2004;23:1239-47.
- Liu S, Gu X, Zhu L, et al. Effects of propofol and sevoflurane on perioperative immune response in patients undergoing laparoscopic radical hysterectomy for cervical cancer. *Medicine (Baltimore)* 2016;95:e5479.
- Hanprasertpong J, Jiamset I, Geater A, et al. Clinical Aspects and Prognostic Factors for Survival in Patients with Recurrent Cervical Cancer after Radical Hysterectomy. *Oncol Res Treat* 2016;39:704-11.
- Kyo S, Kato T, Nakayama K. Current concepts and practical techniques of nerve-sparing laparoscopic radical hysterectomy. *Eur J Obstet Gynecol Reprod Biol*

- 2016;207:80-8.
22. Yang Y, Qin T, Zhang W, et al. Laparoscopic nerve-sparing radical hysterectomy for bulky cervical cancer (>=6 cm) after neoadjuvant chemotherapy: A multicenter prospective cohort study. *Int J Surg* 2016;34:35-40.
 23. Takatori E, Shoji T, Takada A, et al. A retrospective study of neoadjuvant chemotherapy plus radical hysterectomy versus radical hysterectomy alone in patients with stage II cervical squamous cell carcinoma presenting as a bulky mass. *Onco Targets Ther* 2016;9:5651-7.
 24. Li WP, Liu H, Chen L, et al. A clinical Comparison of Lobaplatin or Cisplatin with Mitomycin and Vincristine in Treating Patients with Cervical Squamous Carcinoma. *Asian Pac J Cancer Prev* 2015;16:4629-31.
 25. Wang JQ, Wang T, Shi F, et al. A Randomized Controlled Trial Comparing Clinical Outcomes and Toxicity of Lobaplatin- Versus Cisplatin-Based Concurrent Chemotherapy Plus Radiotherapy and High-Dose-Rate Brachytherapy for FIGO Stage II and III Cervical Cancer. *Asian Pac J Cancer Prev* 2015;16:5957-61.
 26. Li X, Ran L, Fang W, et al. Lobaplatin arrests cell cycle progression, induces apoptosis and alters the proteome in human cervical cancer cell Line CaSki. *Biomed Pharmacother* 2014;68:291-7.
 27. Kirpensteijn J, Teske E, Kik M, et al. Lobaplatin as an adjuvant chemotherapy to surgery in canine appendicular osteosarcoma: a phase II evaluation. *Anticancer Res* 2002;22:2765-70.
 28. Wu Q, Qin SK, Teng FM, et al. Lobaplatin arrests cell cycle progression in human hepatocellular carcinoma cells. *J Hematol Oncol* 2010;3:43.
 29. Yin CY, Lin XL, Tian L, et al. Lobaplatin inhibits growth of gastric cancer cells by inducing apoptosis. *World J Gastroenterol* 2014;20:17426-33.
 30. Wang Y, Zheng WL, Ma WL. Lobaplatin inhibits the proliferation of hepatocellular carcinoma through p53 apoptosis axis. *Hepat Mon* 2012;12:e6024.
 31. Lee SJ, Hwang SO, Noh EJ, et al. Transactivation of bad by vorinostat-induced acetylated p53 enhances doxorubicin-induced cytotoxicity in cervical cancer cells. *Exp Mol Med* 2014;46:e76.
 32. Matsumoto M, Nakajima W, Seike M, et al. Cisplatin-induced apoptosis in non-small-cell lung cancer cells is dependent on Bax- and Bak-induction pathway and synergistically activated by BH3-mimetic ABT-263 in p53 wild-type and mutant cells. *Biochem Biophys Res Commun* 2016;473:490-6.

Cite this article as: Sun W, Zhao X, Lu Z, Guo Q. *P53* introduction enhances chemotherapy-induced apoptosis in HeLa cells. *Transl Cancer Res* 2018;7(4):1103-1111. doi: 10.21037/tcr.2018.08.25